Supplementary Material, Slean *et al*.

Content

I. Figure S1: Slipped-DNAs and DNA metabolism

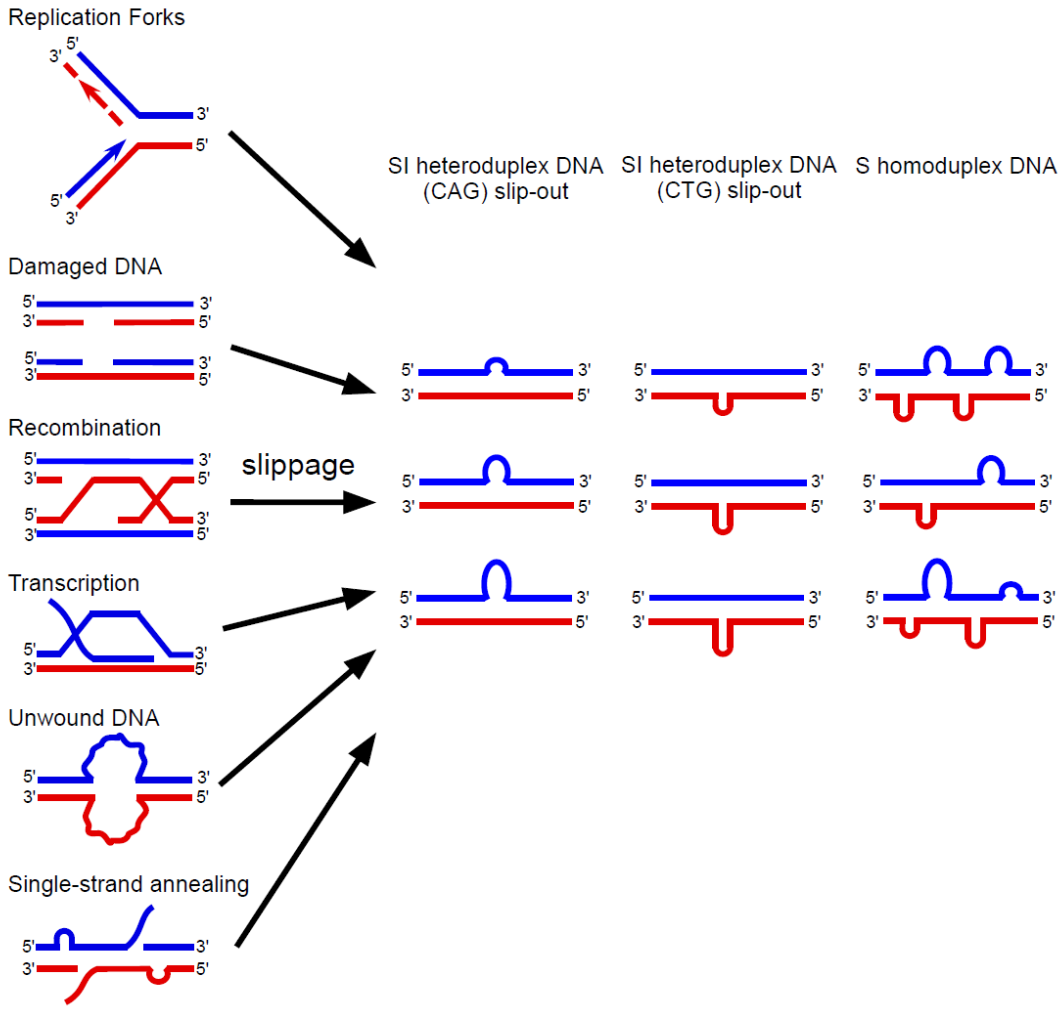

Figure S1: Slipped-DNAs can form during a variety of DNA metabolic processes. Slip-outs of various lengths can be composed of either CAG or CTG repeats in the case of Slipped Intermediate (SI) heteroduplex DNA, or both CAG and CTG repeats in the case of Slipped (S) homoduplex DNA

Figure S2: Interconversion of Junction forms

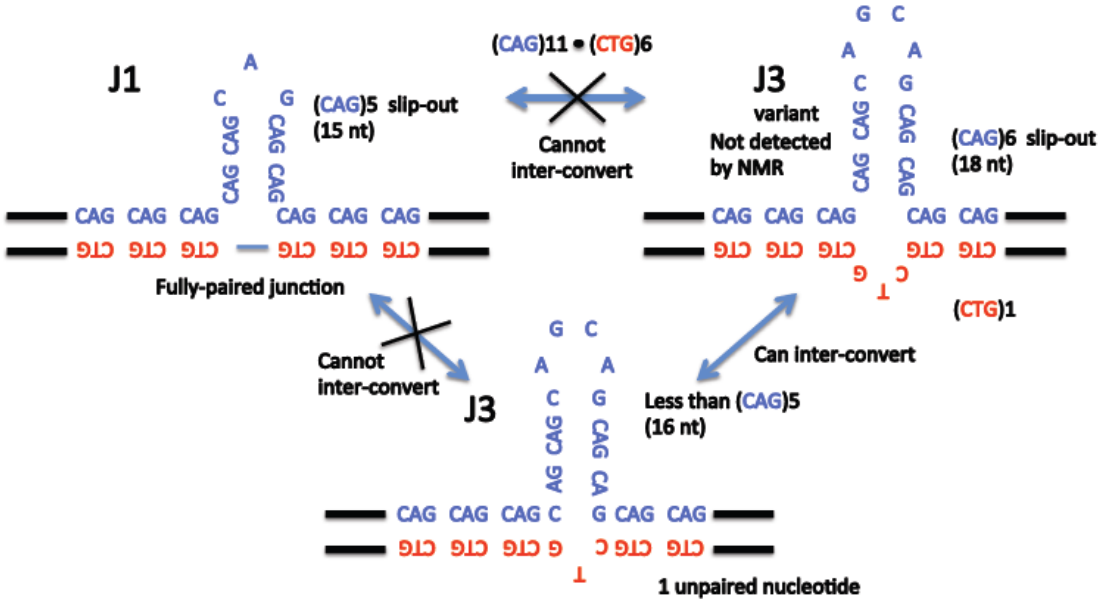

Figure S2: The fully-paired J1 junction cannot easily interconvert to the 1-unpaired nucleotide J3 junction (which is equivalent to a 3-unpaired nucleotide form) due to the energy needed to break all hydrogen bonds between all base pairs in the slip-out and many base pairs in at least one arm of the complementary base paired repeats. NB: a 3-unpaired nt J3 variant would be similar to a J1 junction, but hybridized out-of-register by one repeat unit (across from the slip-out); however this J3 variant is not seen by NMR. The same applies to the J4 and J6 conformations. An example of a slipped-DNA with (CAG)11·(CTG)6 is shown.

II. Figure S3: Oligos modeling junctions run on a denaturing gel (left) and native gel (right)

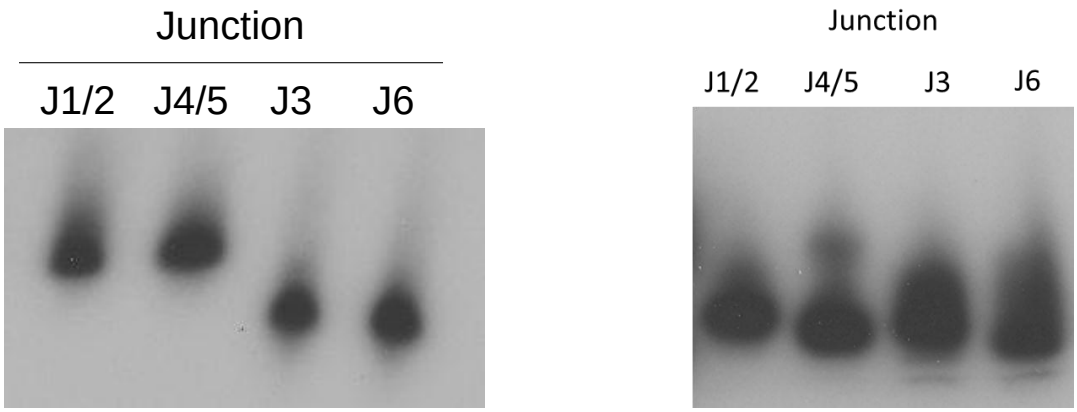

Figure S3: Electrophoretic migration of junction model oligos on a 5% denaturing acrylamide gel (left). Each oligo migrates as a single band, unlike on native acrylamide (right).

III. Trinucleotide repeat junctions selected for NMR structural studies

In Fig. 1B an overview is given of the triplet repeat junction models selected for NMR structural studies, the sequences are listed in Table S1. Below the sequence, the most likely stacking of the arms in the three-way junction conformation is given; these stacking preferences are based on the loop and pyrimidine rules proposed by van Buuren *et al*. J. Mol. Biol., 2000 (20) and/or Wu *et al*. NAR, 2004 (25). The loop and pyrimidine rules that predict the stacking of the arms in a three-way junction are described and exemplified for J4/5 in section "**V. Junction 4/5 - supplementary information for Figure 2; *Schematic of J4/5 and stacking of the arms"***.

Table S1: *DNA trinucleotide repeat junction model sequences selected for NMR structural studies.* The trinucleotide repeats are highlighted in bold. Table S1 also gives for each sequence a prediction of conformation based on the three-way junction loop and pyrimidine rules (van Buuren et al., J.Mol. Biol. 2000 (20); Wu et al. NAR 2004 (25)). The schematic explaining the selection rules is shown in Figure S4. These rules predict whether the three-way junction sequence will fold with a single conformation with I:III or I:II arm stacking or if it will remain non-stacked and/or display multiple conformations (see Fig. 2 for I/II/III arm designations). All junctions are predicted to display multiple conformations. Here we present the NMR data for J1/2, J3, and J4/5; the NMR data for J6 will be presented elsewhere. These sequences are the same as those presented in Figure 1B. In the table below each nucleotide has been numbered from the 5' end to the 3' end. Nucleotides expected to participate as CAG and CTG repeat units at the junction/slip-out are indicated in blue and red fonts, respectively. The 5'-CTTG-3' expected to be at the intra-strand hairpin tips as well-defined H2-type CTTG loops, for which characteristic resonances are well established in NMR spectra (Wu et al. NAR 2004 (25)), are in green font.

*The free energies of the various conformations were derived using the program DNAmelt (Zuker, M. *Mfold web server for nucleic acid folding and hybridization prediction*. NAR (2003) 31 (13): 3406-15; SantaLucia, Jr. *A unified view of polymer, dumbbell, and oligonucleotide DNA nearest-neighbour thermodynamics.* PNAS (1998) 95: 1460-1465). Evidently, all proposed conformations (e.g. the set J1, J2, J1/2_1, J1/2_2 and the set J4, J5, J4/5_1, J4/5_2 and also J3 see Figure 2) are thermodynamically quite close and may thus all appear.

Name	Sequence
Junction 1/2	5'-$G_1C_2G_3C_4$**$C_5A_6G_7C_8A_9G_{10}$**$G_{11}C_{12}$-$C_{13}T_{14}T_{15}G_{16}$- $G_{17}C_{18}$**$C_{19}A_{20}G_{21}C_{22}A_{23}G_{24}$**$G_{25}$-$C_{26}T_{27}T_{28}G_{29}$- C_{30}**$C_{31}T_{32}G_{33}C_{34}T_{35}G_{36}$**$G_{37}C_{38}G_{39}C_{40}$-3' Stacking prediction based upon loop and pyrimidine rules: conf J1: **non-stacked**; conf J2: **no stacking preference**; conf J1/2_1: **I:II stacking preference**; conf J1/2_2: **I:II stacking preference** *Fig. 2E: NMR conformations are J1 (-10.51 kcal/mol), J2 (-10.04 kcal/mol), J1/2_1 (-12.89 kcal/mol), and J1/2_2 (-13.37 kcal/mol)
Junction 3	5'-$G_1C_2G_3G_4$**$A_5G_6C_7A_8G_9$**$C_{10}C_{11}$-$C_{12}T_{13}T_{14}G_{15}$-$G_{16}G_{17}$**$C_{18}A_{19}G_{20}C_{21}A_{22}$**$C_{23}$- $C_{24}T_{25}T_{26}G_{27}$-G_{28}**$T_{29}G_{30}C_{31}T_{32}G_{33}C_{34}T_{35}$**$C_{36}C_{37}G_{38}C_{39}$-3'

	Stacking prediction based upon loop and pyrimidine rules**:** conf J3: **I:III stacking preference**; conf J3_1: **I:III stacking preference**; conf J3_2: **I:III stacking preference** *Fig. 2F: NMR conformations are J3 (-13.43 kcal/mol), J3_1 (-13.80 kcal/mol), and J3_2 (-13.63 kcal/mol)
Junction 4/5	5'-$G_1C_2A_3C_4$**$C_5A_6G_7C_8A_9G_{10}$**G_{11}-$C_{12}T_{13}T_{14}G_{15}$-C_{16}**$C_{17}T_{18}G_{19}C_{20}T_{21}G_{22}$**$G_{23}A_{24}$-$C_{25}T_{26}T_{27}G_{28}$-$T_{29}C_{30}$**$C_{31}T_{32}G_{33}C_{34}T_{35}G_{36}$**$G_{37}T_{38}G_{39}C_{40}$-3' Stacking prediction based upon loop and pyrimidine rules: conf J4: **non-stacked**; conf J5: **I:II stacking preference**; conf J4/5_1: **I:III stacking preference**; conf J4/5_2: **I:II stacking preference** *Fig. 2D: NMR conformations are J4 (-9.15 kcal/mol), J5 (-8.59 kcal/mol), J4/5_1 (-10.17 kcal/mol), and J4/5_2 (-10.57 kcal/mol)
Junction 6	5'-$G_1C_2G_3G_4$**$A_5G_6C_7A_8G_9C_{10}A_{11}$**$C_{12}$-$C_{13}T_{14}T_{15}G_{16}$-$G_{17}$**$T_{18}G_{19}C_{20}T_{21}G_{22}$**$C_{23}C_{24}$-$C_{25}T_{26}T_{27}G_{28}$-$G_{29}$**$G_{30}C_{31}T_{32}G_{33}C_{34}T_{35}$**$C_{36}C_{37}G_{38}C_{39}$-3' Stacking prediction based upon loop and pyrimidine rules: **non-stacked**

IV. Overview of main NMR experiments.

Table S2: *Overview of the main recorded NMR spectra*. The spectra aim to assess the main conformational features of the sequences. The set includes 1D NMR spectra together with 2D NOESY spectra in H_2O and in D_2O, as well as TOCSY (2D) recorded in D_2O. The NMR junction ssDNAs were dissolved in 10 mM sodium phosphate pH 6.7 containing 0.1 mM EDTA and 7% D_2O to a DNA concentration of 0.2 to 0.5 mM. The samples were heated at 95°C, snap-cooled in ice-water and transferred to a Shigemi NMR tube. All NMR spectra were acquired at 5 or 25°C using a Varian 600 Inova spectrometer equipped with a shielded triple-axis gradient HCN probe.

Junction 1/2			
Solvent	2D NOESY	2D TOCSY	1 D
H_2O	10^oC/300 ms		10^oC
D_2O	5 mM $MgCl_2$ 30^oC	5 mM $MgCl_2$ $30\ ^oC$	
D_2O	5 mM $MgCl_2$ $40\ ^oC$	5 mM $MgCl_2$ $40\ ^oC$	
Junction 3			
Solvent	2D NOESY	2D TOCSY	1 D
H_2O	10^oC		10^oC
H_2O			20^oC
H_2O			30^oC
H_2O	40^oC		40^oC
H_2O	0.5 mM $MgCl_2$ $10\ ^oC$		0.5 mM $MgCl_2$ $10\ ^oC$
H_2O			1.0 mM $MgCl_2$ $10\ ^oC$

H_2O	2.0 mM $MgCl_2$ 10 °C		2.0 mM $MgCl_2$ 10 °C
H_2O	3.0 mM $MgCl_2$ 10 °C		3.0 mM $MgCl_2$ 10 °C
H_2O			4.0 mM $MgCl_2$ 10 °C
H_2O			5.0 mM $MgCl_2$ 10 °C
H_2O	6.0 mM $MgCl_2$ 10 °C		6.0 mM $MgCl_2$ 10 °C
H_2O			7.0 mM $MgCl_2$ 10 °C
H_2O			8.0 mM $MgCl_2$ 10 °C
H_2O	9.0 mM $MgCl_2$ 10 °C		9.0 mM $MgCl_2$ 10 °C
H_2O			10.0 mM $MgCl_2$ 10 °C
H_2O			11.0 mM $MgCl_2$ 10 °C
H_2O			13.2 mM $MgCl_2$ 10 °C
Junction 4/5			
H_2O	10 °C		10 °C
H_2O			15 °C
H_2O	20 °C		20 °C
H_2O	25 °C		25 °C
H_2O	30 °C		30 °C
H_2O	35 °C		35 °C
H_2O			40 °C
H_2O			45 °C
H_2O			0.5 mM $MgCl_2$ 20 °C
H_2O			0.5 mM $MgCl_2$ 30 °C
H_2O	2.5 mM $MgCl_2$ 10 °C		2.5 mM $MgCl_2$ 10 °C
H_2O			2.5 mM $MgCl_2$ 20 °C
H_2O			2.5 mM $MgCl_2$ 30 °C
H_2O			5.0 mM $MgCl_2$ 10 °C
H_2O	5.0 mM $MgCl_2$ 20 °C		5.0 mM $MgCl_2$ 20 °C
H_2O			5.0 mM $MgCl_2$ 30 °C
H_2O			5.0 mM $MgCl_2$ 40 °C
D_2O	5 mM $MgCl_2$ 20 °C	5 mM $MgCl_2$ 20 °C	
D_2O	5 mM $MgCl_2$ 30°C	5 mM $MgCl_2$ 30 °C	
D_2O	5 mM $MgCl_2$ 40 °C	5 mM $MgCl_2$ 40 °C	
D_2O	10 mM $MgCl_2$ 20°C	5 mM $MgCl_2$ 20 °C	
D_2O	10 mM $MgCl_2$ 40°C	5 mM $MgCl_2$ 40 °C	

V. Junction 4/5 - supplementary information

Supplementary Material for Figure 2; *Schematic of J4/5 and stacking of the arms.*
In three-way junctions the arms are usually stacked and arm stacking preference is guided by two main rules as explained in Fig. S4. Application of these rules to the J4/5 sequence leads to the following outcome. In conformation J5 (see Fig. 2D) a I:II stacked conformation is preferred as it puts a C (C_{20}) in the inner strand of arm I in the penultimate position and leads to arm III being capped by a stable C_{17}-T_{18}//$G_7C_8A_9$-G_{10} tetra-loop (here // indicates a break in the backbone = no phosphate linkage). This conformation is consistent with the NMR data (see also paragraph below). Briefly, the A_9:T_{18} (Fig. 2D) is the closing base pair of this junction tetraloop and shows (if well formed) one cross peak namely to the C_{17}:G_{10} base pair (resonance 1 in Fig. 2C). In this I:II stacked conformation, the A_6:T_{35} base pair is stacked between two C:G basepairs across the junction (C_5:G_{36} and C_{34}:G_{19}), leading to two cross peaks (e.g. resonance 2 in Fig. 2C). Stacking of arms I and III (I:III stack) is less stable, because in this context the G_{33}-residue is located in the penultimate position from the junction in the inner strand of arm I. In addition, the loop capping arm II is less stable, because it has an A (A_6) in the 5'-position in the tetraloop with sequence C_5-$A_6G_7C_8$//T_{35}-G_{36}. The additional cross peaks, seen for instance in Fig. 2A, 2B, and 2C, show that more than two conformations occur. Further alternate conformations of J4 and J5, conformations such as J4/5_1 and J4/5_2, can thus potentially also occur; the particular conformations J4/5_1 and J4/5_2 are consistent with the NMR spectra (see below). For J4, J4/5_1 and J4/5_2, similar considerations can be put forward to describe their folded and/or stacked forms.

Figure S4

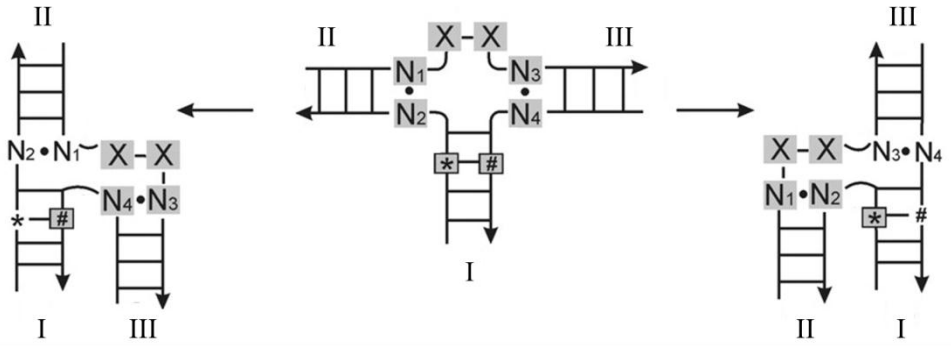

Figure S4. *Schematic of the folding of three-way junctions from their open form (middle) into the two stacked forms (left and right).* The stacked forms are preferred over the open form. Selection of the stacked form I:II or I:III depends on sequence and is guided by the following two main selection rules that have been proposed (van Buuren et al., J. Mol. Biol., 2000 (20); Wu et al., NAR 2004 (25)). I) Loop rule: The non-stacked arm should be capped at the junction with a stable loop, e.g. a tetraloop that starts with a pyrimidine and the same holds for a tri-loop. II) Pyrimidine rule: A pyrimidine should be located in the penultimate position of the junction in arm I (boxed residue). In the text we adhere to the Altona notation (61) for the arms, i.e. arm I/arm II/arm III, to indicate the usual stacking of the two of the arms of the three-way junction.

Junction 4/5; interpretation of imino resonance NMR data.
As described in the main text, the 2D TOCSY and 2D NOESY NMR spectra of J4/5 demonstrate the formation of a three-way junction with well-formed arms but with formation of multiple conformations around the junction. Here we give a consistent interpretation and assignment of the imino regions of the NMR 2D NOESY. The conformations are summarized in Fig. 2D, the NMR data are shown in Figures 2A, 2B and 2C (and Fig. S5), and the obtained resonance assignments are given in Table S3A.

First, we note that the arms are well formed as follows from the presence of characteristic NMR resonances for the CTTG loops (see main text); the presence of well-formed arms is confirmed by the imino spectrum which provides evidence for the presence of an A_3:T_{38} base pair and an A_{24}:T_{29} base pair, each flanked by two G:C base pairs. With regard to the A_3:T_{38} base pair: In the imino region of the 2D NOESY of J4/5 (Fig. 2B and 2C) imino resonance 4 can be assigned to T_{38} (arm II in both J4 and J5, Fig. 2C), because it shows, together with one of its contacted G-imino resonances, a cross peak to a Me-proton resonating at 1.38 ppm, a shift corresponding to a T in a GTG sequence (Fig. 2B). Consistent with A_3:T_{38} being flanked by two G:C base pairs, resonance 4 shows two cross peaks to G iminos in C:G base pairs. With regard to the A_{24}:T_{29} base pair: Consistent with the presence of an A_{24}:T_{29} base pair, we find at the resonance 4 imino resonance position NOE contacts to Me-protons resonating at ~1.6 ppm (Fig. 2B) shift values that correspond to a T in a CTG sequence (this additional imino is designated resonance 4' for convenience further on). These A:T imino resonances thus provide, together with the characteristic Me/H6 resonances of CTTG H2-type tetra-loops (Fig. 2A), full evidence for the formation of a three-way junction with well-formed helical arms.

In addition to these A:T imino resonances, further A:T resonances are observed. 1) A further A:T imino resonance is seen at the resonance 4 (/ 4') position (designated resonance 3). 2) This A:T resonance 3 shows an exchange cross peak with another A:T imino resonance (resonance 2). Resonance 3 (and 4') shows together with the G imino resonances of the flanking G:C base pairs a multitude of contacts with Me-protons at ~1.6 ppm and thus to T-Me's in CTG sequence elements. This indicates multiple conformations for these CTG elements and thus for the junction, as these sequence elements are located at and around the junction (see also main text). 3) In addition, a weak A:T imino resonance 1 is observed.

With these data, a consistent interpretation of the J4/5 NMR data can be made, namely the data are consistent with J5 being in exchange with J4 and other conformations (Fig. 2D). In its most likely conformation, arms I and II of J5 are stacked. Base pair A_6:T_{35} (Fig. 2D) in arm II is then flanked by two C:G base pairs of which one is located across the junction. The imino resonance 2 in the NMR spectrum (Fig. 2B and 2C) can then be assigned to T_{35} in A_6:T_{35} in the J5 I:II-stacked conformation and resonance 3 can be assigned to T_{35} in A_6:T_{35} in J4 (Fig. 2D); this thus nicely explains the exchange cross peak between these two resonances and the observation that both are flanked by two C:G base pairs. Moreover, each shows an NOE contact to a T-Me in a CTG sequence (characteristic ~1.6 ppm resonance position). In the J5 I:II-stacked conformation, one finds in addition the base pair A_9:T_{18} (Fig. 2D). It is part of the junction loop - $C_{17}T_{18}$//$G_7CA_9G_{10}$- and thus is flanked by only one G:C base pair (here // indicates the break in the backbone). This explains the weak imino resonance 1, which shows an NOE contact to T-Me (Fig. 2B) in a CTG sequence. In the J4 conformation, the open planar conformation may

form (arms I to III are unstacked), which leads to partial opening of the ultimate or penultimate base pairs (A_9:T_{18}; A_6:T_{35}). Alternatively, a stacked conformation may form part of the time, for instance with arms I and II stacked, which forces formation of a $T_{18}G_{19}$//C_8A_9 loop capping arm III (here // indicates the break in the backbone). The A_9:T_{18} base pair is then likely to be open at least part of the time and hence highly unlikely to generate an imino resonance; note that already a ~5% open conformation obliterates an imino resonance. We note that the loop and pyrimidine rules (25) suggest that the conformation of J4 considered here with arm I and II stacked is preferred over the one with arm I and III stacked. The net result of the conformational exchange between J5 and J4 is then that one observes only one single resonance for the A_9:T_{18} base pair, namely resonance 1, which corresponds to T_{18} in A_9:T_{18} in the J5 conformation (see above). Of course, the J4 to J5 exchange leads in addition to the above also discussed exchange cross peak between resonance 3 (J5; A_6:T_{35}) and resonance 2 (J4; A_6:T_{35}). The above description fully explains the imino spectrum observed.

Finally, exchange from e.g. J5 may take place to the J4/5_2 conformation (Fig. 2D), which either folds into the I:II or the I:III stacked conformations, of which the I:II stack is more likely to occur based on the loop and pyrimidine rules (25). The unstable T_{32}:T_{21} non-canonical base pair likely induces a more open junction and/or loop conformation in either stacked forms of J4/5_2. Consequently, the A_9:T_{18} (resonance 1 in J5) is in J4/5_2 in the I:II or II:III stacked conformations likely in an open conformation part of the time, so that an imino resonance in the NMR spectrum may not be formed. In J4/5_2, the other base pair, A_6:T_{35}, remains sandwiched between C:G basepairs and lies even further down into arm I, when comparing J4/5_2 and J5. In J5, T_{35} is assigned to resonance 2 (see above) and may exchange then to resonance 3 in J4/5_2. Alternatively, exchange may occur to the J4/5_1 conformation, which shows no preference for any of the two stacked conformations; however, the I:II stacked conformation leads to a less stable T:T base pair being in the coaxial stack (~-0.25 kcal/mol) while the I:III stacked conformation has a more stable A:T base pair in this position (~-2.0 kcal/mol) suggesting that the I:III stacked conformation is more stable. The unstable T_{32}:T_{21} non-canonical base pair likely induces a more open junction and/or loop conformation in either stacked forms of J4/5_1. Consequently, the A_6:T_{35} base pair in arm II (J4; A_6:T_{35}, resonance 3, see above), which in J4 or J5 is flanked by C:G basepairs (see above), may be in exchange with a conformation where it is not flanked by C:G base pairs and likely to be rather open and thus absent in the NMR spectrum (J4/5_1; Fig. 2D). The A_9:T_{18} base pair in arm III of J4/5_1 (A_9:T_{18} is absent in J4, see above, and is resonance 1 in J5) does attain a slight change in its local environment when going from, for instance, J5 to J4/5_1. In J4/5_1, the A_9:T_{18} base pair lies in stem III flanked by two C:G base pairs, which leads to a closed conformation and an additional T_{18} imino resonance with cross peaks to C:G resonances. Resonance 1 is found to be weak and not to show cross peaks, including exchange cross peaks, suggesting a low population of the J4/5_1 state.

The above provides a consistent and minimal interpretation of the imino resonances seen in the NMR spectrum in terms of four specific physically realistic conformational states, each with their own stacked and open conformational substates.

VI. Junction 1/2 - supplementary material, interpretation of imino spectrum

For J1/2 multiple conformations are indicated by the following two key NMR observations (the conformations are summarized in Fig. 2E, the NMR data in Fig. S6, and the resonance assignments in Table S3B). Firstly, five imino A:T resonances are observed (numbers 1, 2, 3, 4, and 5 in Fig. S6). One expects two A:T imino resonances for J1. Thus, multiple conformations are present. Resonance number 1, 2, 3, and 4 are from A:T base pairs that are sandwiched between two G:C basepairs. A consistent interpretation is that the A:T basepair in arm III (J1; A:T flanked by two C:G basepairs) is in exchange with a conformation where it is not flanked by C:G basepairs (J1/2_1), while in arm I of J1 an additional C:G base pair is formed (arm I becomes arm III in J1/2_1). As a consequence, the A:T base pair in arm II (J1) stays flanked by two C:G basepairs in both conformations, but attains a slight change in its local environment leading to the additional resonance. This forms the first potential conformational exchange and explains the extra set of two resonances (A:T resonances 1 & 3 or A:T_1 vs A:T_3). The same considerations but with arms II and III switched, lead to one more set of conformations and resonances (conformations J1 vs J1/2_2; A:T resonances 2 & 4 or A:T_2 vs A:T_4). In addition, the A:T resonances 1 to 4 each show cross peaks to the Me region with methyls at chemical shifts of 1.50 to 1.65 ppm, confirming that the T's in the A:T base pairs are all from a CTG sequence. Secondly, an A:T imino resonance of low intensity is observed (A:T_5). This resonance shows no imino-imino cross peaks, indicating an open conformation as in conformation J2 (A:T only flanked by C:G on one side). Cross-peaks to the H2 region and to the T-Me region are seen, with T-Me near 1.85-1.9 ppm, consistent with a partially non-stacked conformation for the T in the base pair. From the above, it follows that the junction folds into multiple conformations, i.e. at least four conformations are present. The inter-conversion is in the slow-exchange regime, i.e. lifetime of the conformational states is milliseconds or longer. The low intensity of A:T_5 shows that J2 is much less populated than J1 (and its substates, J1/2_1 and J1/2_2).

VII. Junction 3 - supplementary info, interpretation of imino and related NMR spectra

Towards understanding the structure of a slipped-junction with the potential to have a single unpaired nucleotide opposite the slip-out, we consider J3 (Fig. 1B, Table S1, and the NMR data is summarized in Table S3C and in Fig. S7). In this junction, T_{32} is the T present in the CTG opposite the predicted CAG slip-out. The NMR spectra indicate three-way junctions with CTTG loops capping the arms. Most interestingly, the spectra reveal the presence of multiple conformations as illustrated by the following key observations. Five imino A:T resonances are observed (numbered 1, 2a, 2b, 3, and 4; Fig. S7) of which 3 are from A:T basepairs flanked by two C:G base pairs, while the remaining two are from A:T basepairs flanked by only one C:G base pair. A single conformation would have yielded two A:T resonances where each A:T base pair is flanked by two C:G base pairs. Consequently, there must be multiple conformations present.

A more detailed description of the NMR imino spectra provides more insight into the nature of the main and additional conformations of J3. Note first that resonance number 1 and 2b are of A:T basepairs sandwiched between C:G basepairs and in exchange (Fig. S7). Resonance number 2a is from an A:T basepair that is also sandwiched between two C:G basepairs, but shows no exchange. Number 4 shows contact to one C:G basepair, while number 3 has low intensity and a contact to a C:G pair is not visible. These imino resonance data can be interpreted as follows in terms of conformations: In addition to the J3 conformation, which is the conformation for the CAG slip-out and a bulged-out T (T_{32}) in the opposite CTG strand (Fig. 2F), there appear to be at least two extra conformations, namely J3_1 and J3_2 (Fig. 2F). These extra conformations have either a A_8:T_{32} basepair (J3_1) or A_{19}:T_{32} (J3_1) basepair and are each flanked by only one C:G basepair. These extra conformations explain the presence of resonances number 3 and 4, which show only one cross peak. Resonance 2a, which is from an A:T basepair flanked by two C:G basepairs, but with no exchange can be attributed to basepair A_5:T_{35}. The base pair A_5:T_{35} is in the middle of stem III in the J3 conformation (Fig. 2F) or is located in stem I in either the J3_1 or the J3_2 conformation. The A_5:T_{35} basepair is thus not affected much by the conformational exchange processes at the junction. Consequently, it leads to a single relatively intense resonance with contacts to two C:G resonances (Table S3C). Resonances 1 and 2b, that is each from an A:T basepair between two C:G basepairs and with exchange to each other, can be attributed to A_{22}:T_{29}. Exchange of the J3_1 conformation to the J3 conformation leads to 1 to 2b cross peak exchange. Exchange of the J3_2 conformation to the J3 conformation leads also to the 1 to 2b cross peak exchange. The J3_1 and J3_2 conformations, in which either A_{19}:T_{32} may form or A_9:T_{32}, and the J3 conformation lead to at least three basic conformations, which each may fold into I:II-stacked, I:III-stacked, and ‘non-stacked’ conformations.

VIII. Resonance assignment Tables for J1/2, J3 and J4/5

Table S3A: (J4/5) Characteristic Thymine H6 and CH3 chemical shifts of the H2-type CTTG loop and tentative assignments of J4/5 resonances (H6, H5, H2, imino H3).

CTTG Loop	Resonance	J4/5					Standard TWJ1	
		H6	CH3				H6	CH3
Loop1	T_{13}	7.87	1.99				7.94	2.04
	T_{14}	7.56	1.32				7.59	1.33
Loop2	T_{26}	7.84	2.01				7.84	2.00
	T_{27}	7.53	1.29				7.53	1.28
CTG -4 ~12 res'nces		7.17-7.61	1.38-191					
CTG - stem B	T_{18}	id.	id.					
CTG	T_{21}	Id	Id					
CTG	T_{32}	Id	Id					
CTG stem A	T_{35}	7.43	1.53				7.43(6)	1.53(4)
Imino		T-H3	G-H1	G-H1	H2	Assignment	Base Pair	Note
A:T	1	14.15			7.68	T_{18}	A_9:T_{18}	Exch
A:T	2	13.95	12.85	12.78	7.59	T_{18}	A_9:T_{18}	3 / 4 to 2
A:T	3	13.80	12.88	12.67		T_{18}	A_9:T_{18}	
A:T	4	13.78	12.93	12.78	7.80	T_{35}	A_6:T_{35}	

Table S3B: (J1/2) Thymine H3 (imino), Methyl and H2 tentative chemical shifts

Imino	Resonace	T-H3	G-H1	GH1	Me	H2	Assignment	Base Pair	Note
									Consistent With; conf
A:T	1	13.99	12.98	12.72	*1.55*	*7.58*	T_{35}	A_6:T_{35}	CTG-J1/2_1
A:T	2	13.96	12.93	12.71	*1.55*	*7.58*	T_{32}	A_{23}:T_{32}	CTG-J1/2_2
A:T	3	13.80	12.99	12.65	*1.62*	*7.50*	T_{35}	A_6:T_{35}	CTG-J1
A:T	4	13.75	12.85	12.64	*1.58*	*7.50*	T_{32}	A_{23}:T_{32}	CTG-J1
A:T	5	14.07			*1.87*	*7.60*	T_{32}/ T_{35}		(semi) non stacked; J2

Table S3C: (J3) Thymine H3 (imino) tentative chemical shifts

Imino	Resonance	T-H3	G-H1	GH1	Assignment	Base Pair	Note
A:T	1	13.97	12.85	12.80	T_{29}	A_{22}:T_{29}	Exch 1 to 2b
A:T	2b	13.88	12.85	12.80	T_{29}	A_{22}:T_{29}	
A:T	2a	13.90	12.90	12.72	T_{35}	A_{5}:T_{35}	
A:T	3	13.75				A_{19}:T_{32}	
A:T	4	13.67	12.82		T_{32}	A_{8}:T_{32}	

IX. Resonance assignment NMR spectra figures for J1/2, J3 and J4/5

Figure S5A: (J4/5) The H5-H6 correlations in the 2D TOCSY of J4/5 annotated for clarification. Over 15 resonances are observed for the 13 cytosine residues in the sequence, indicating multiple conformations.

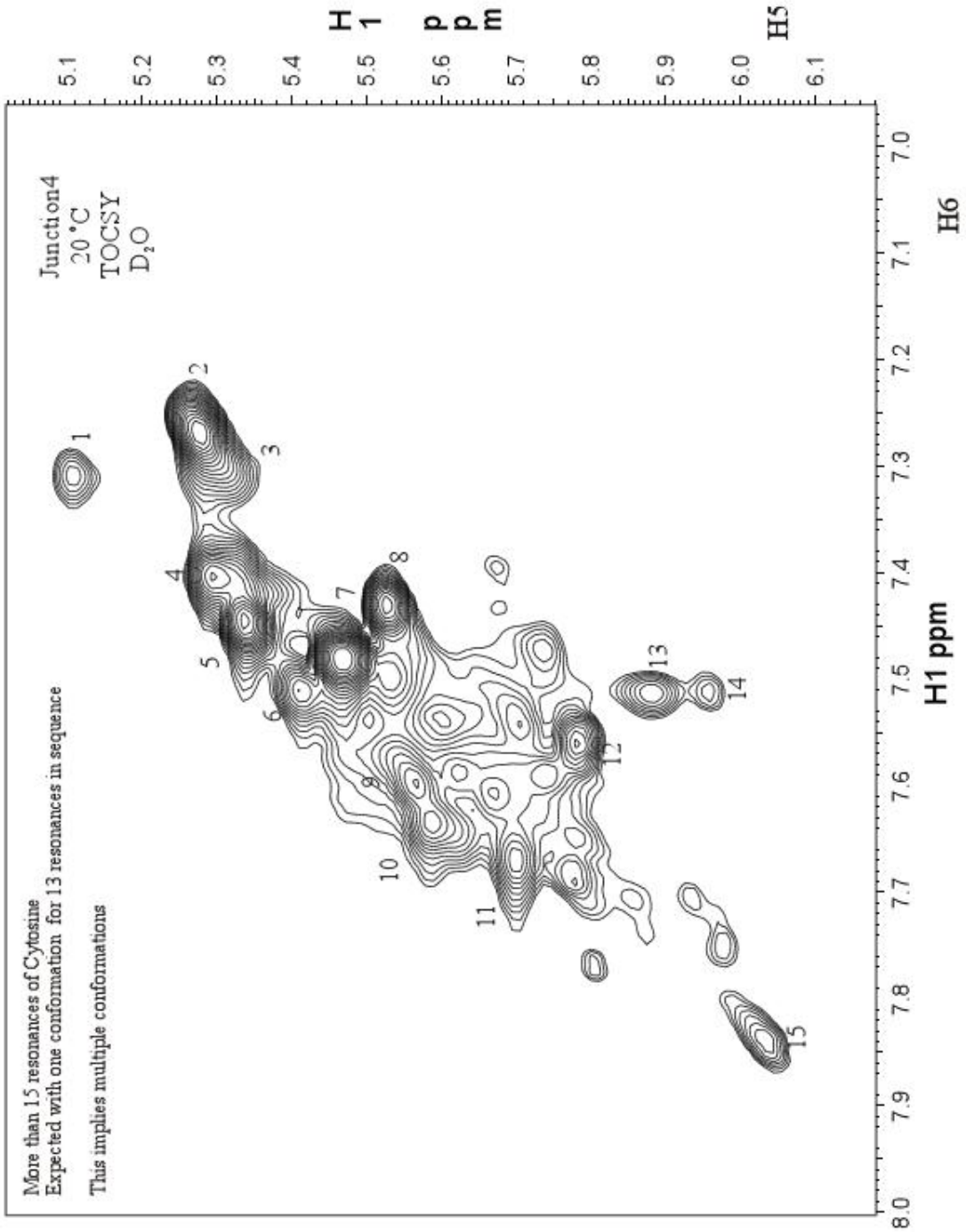

Figure S5B: (J4/5) Imino-H2 region in the 2D NOESY of J4/5, annotated for clarification. The intra-residue contacts between thymine iminos in A:T base pairs and H2 are indicated as well as the contacts of these H2's to the sequential G imino in G:C base pairs.

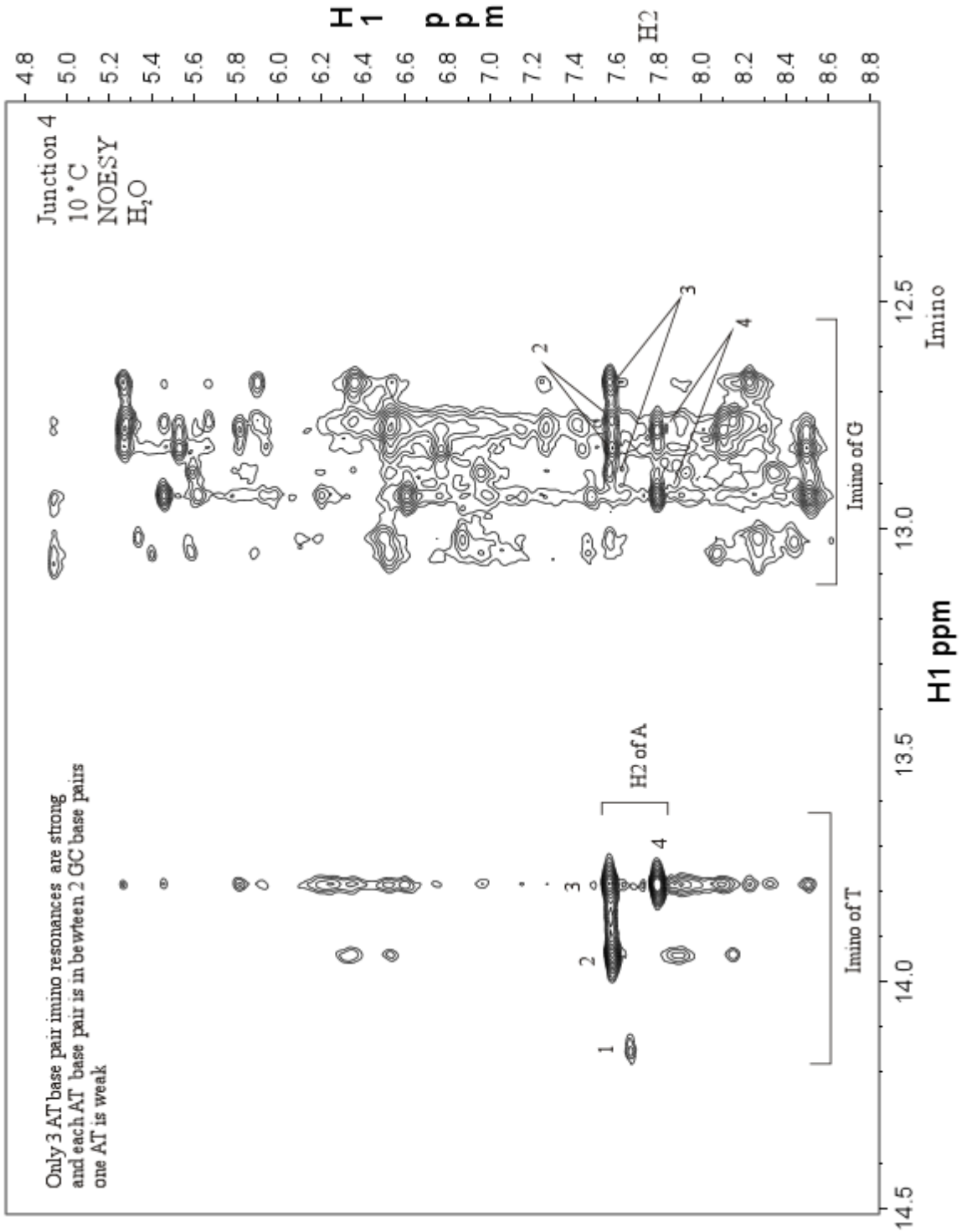

Figure S6A: (J1/2) The imino section of the 2D NOESY spectrum of J1/2 (10 °C, 300 ms mixing time) annotated for clarification. Only 2 A:T base pairs are present in the sequence, while four A:T resonances are evident, implying multiple conformations.

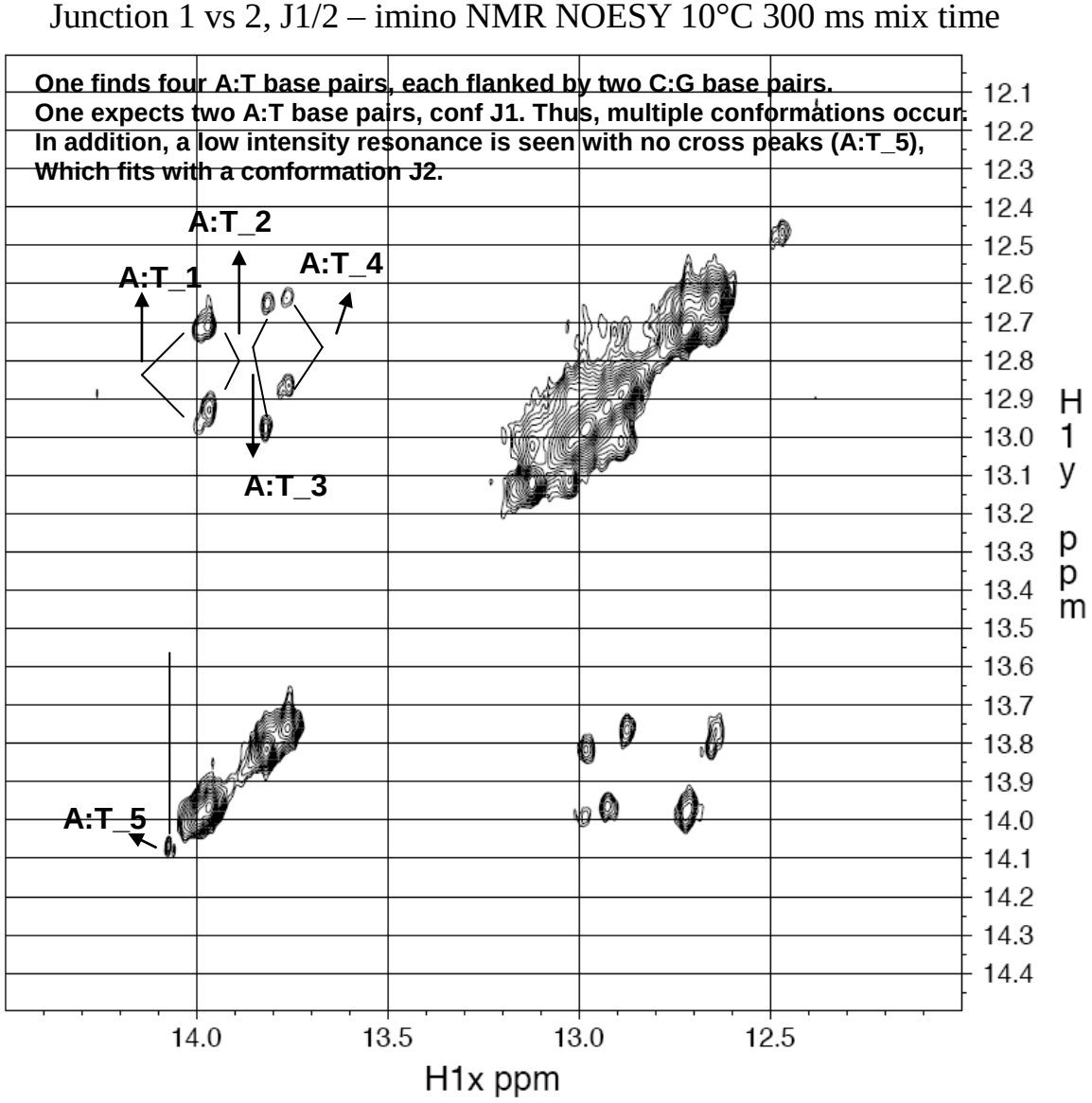

Figure S6B: (J1/2) Imino-H2 region (bottom) and imino-Me region (top) in the 2D NOESY of J1/2, annotated for clarification. The intra-residue contacts between thymine iminos in A:T base pairs and H2 are indicated as well as the contacts of these H2's to the sequential G imino in G:C base pairs.

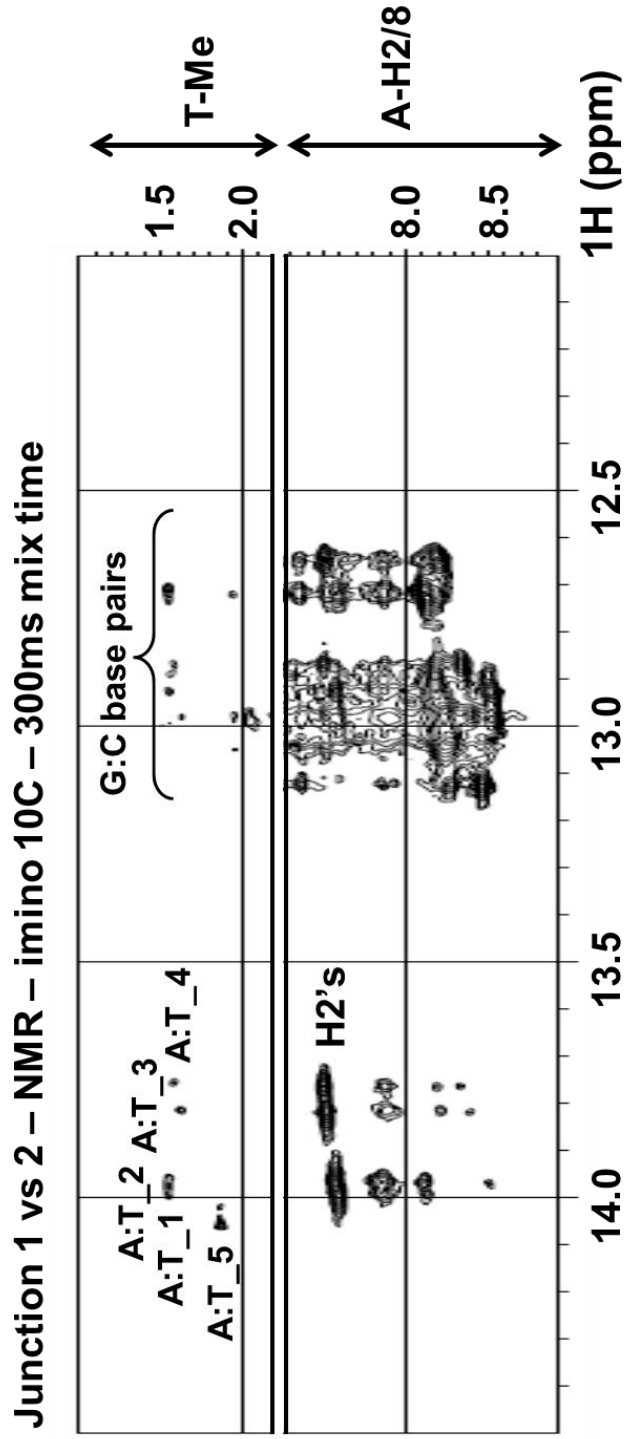

A:T imino (and G:C imino) connects to T-methyl at 1.52-1.65 ppm, showing that the T's are located in the CTG sequence and thus that A:T are in the stem.

Figure S6C: (J1/2) The imino to Thymine-Me section of the same 2D NOESY (10 C, 300 ms, 600 MHz), annotated for clarification. The A:T imino resonances (and of G:C base pairs) connect to Thymine-Me at 1.52 ppm to 1.65 ppm, showing that the Thymine residues in the A:T base pairs are located in a CTG sequence and thus belong to the A:T base pairs in the stems (see main text).

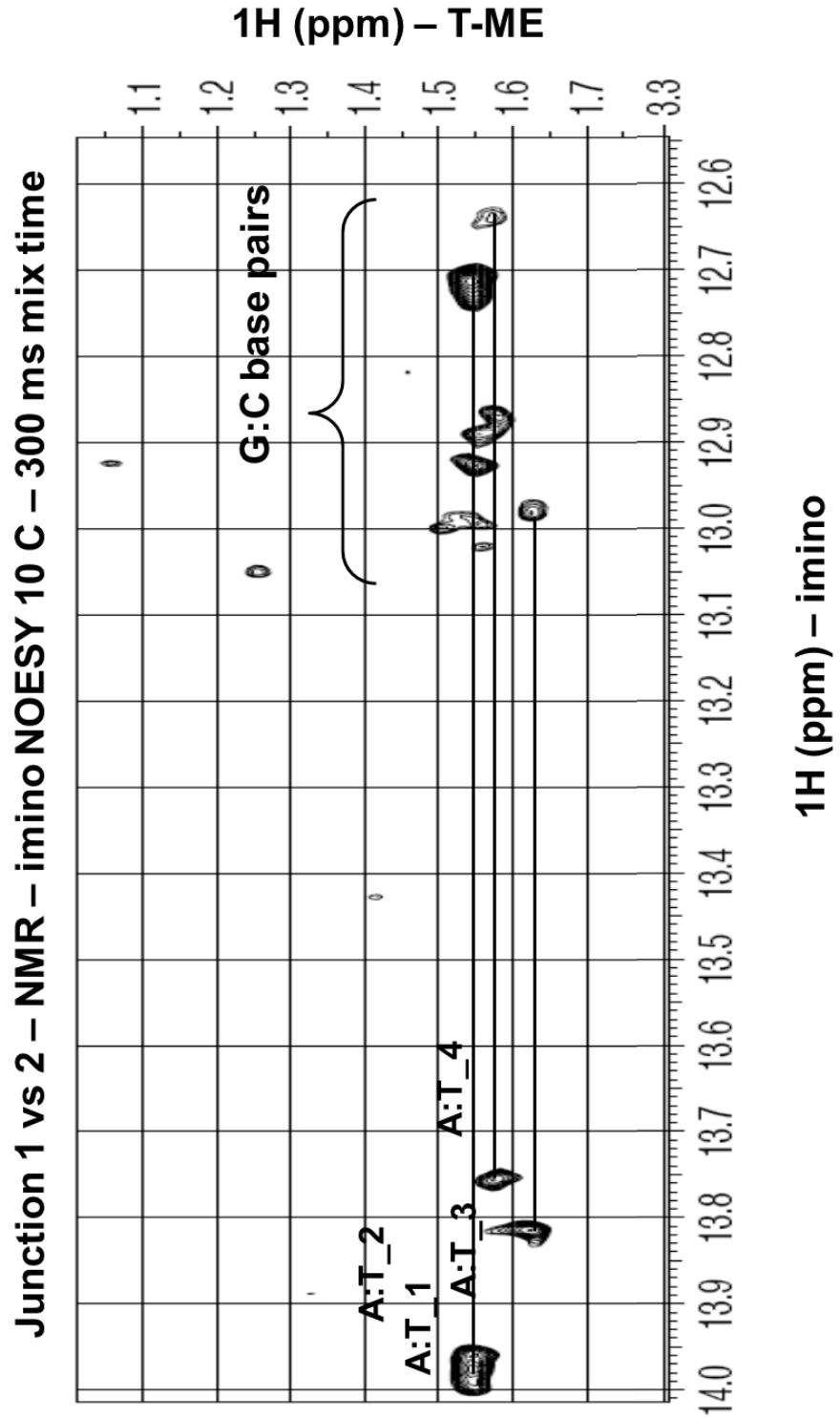

Figure S7: (J3) The imino section of the 2D NOESY spectrum of J3 annotated for clarification. Only 2 A:T base pairs are present in the sequence, while four A:T resonances are evident, implying multiple conformations. In addition, an exchange cross peak is observed between the A:T resonances 1 and 2a/b.

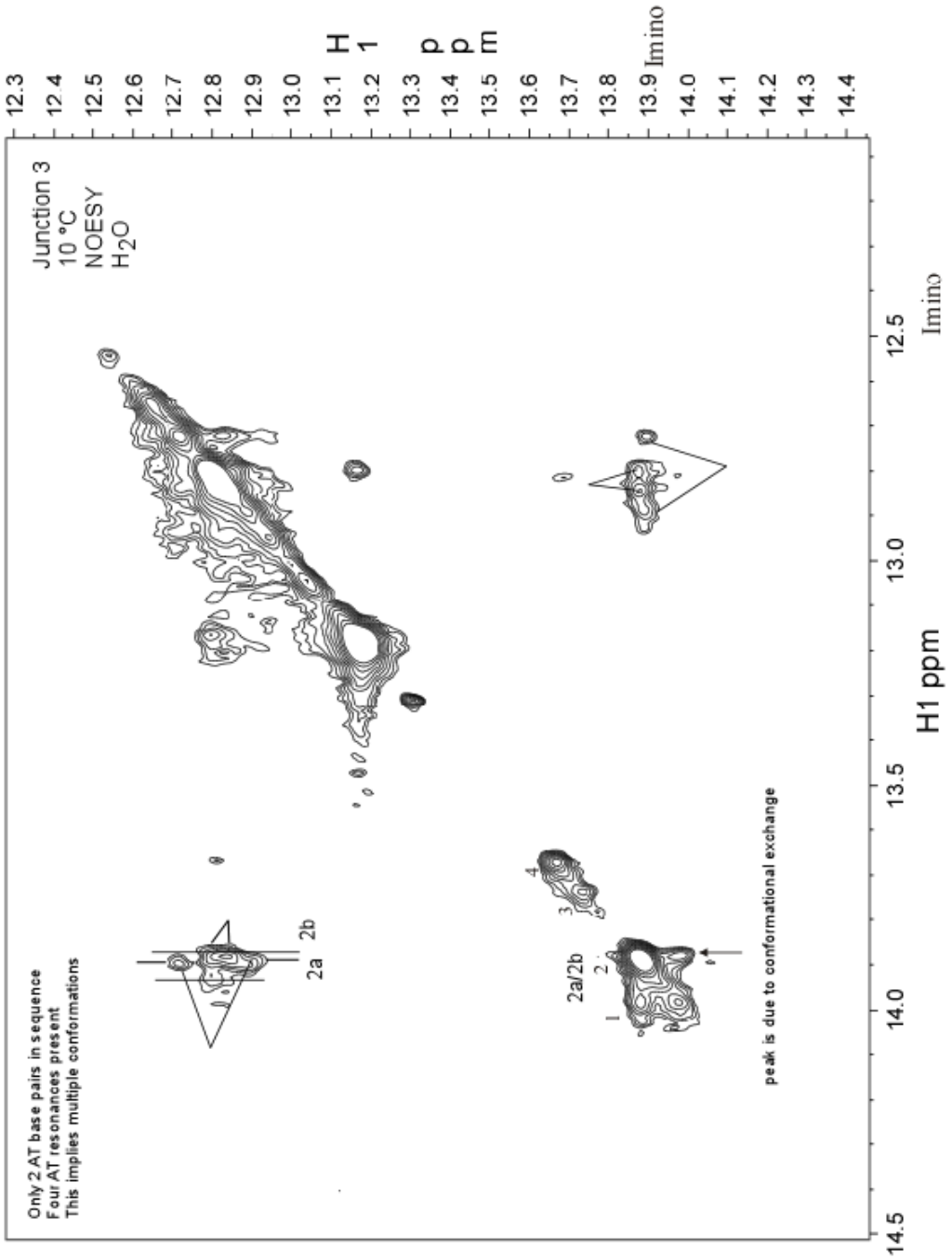

X. Figure S8: Mapping of junction cleavage by XPF-ERCC1

End-labeled junctions were incubated with XPF/ERCC1 as described in the main text and run alongside Maxam-Gilbert chemical sequencing ladders on a denaturing acrylamide gel. Gel was dried and exposed to X-ray film. Arrows indicate sequence cleavage sites.

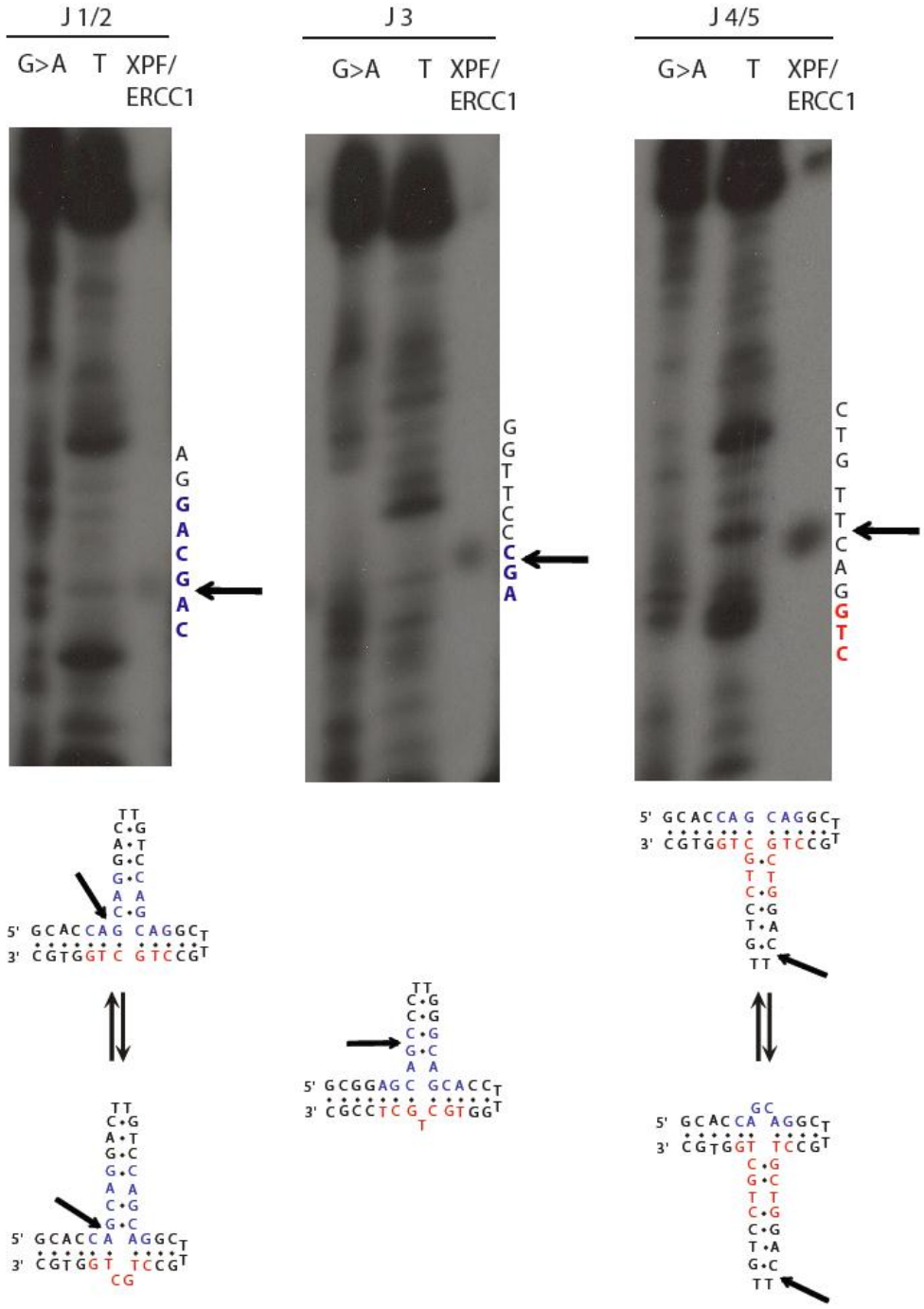

XI. Figure S9: Repair of junction structures by mismatch repair deficient cell extracts

Slipped Junction repair substrates p-J1, p-J3 and p-J1/2 were processed using mismatch repair-deficient LoVo cell extracts and repair efficiencies calculated as outlined in the main text. Graph shows that differences in repair of junctions are independent of MMR (repair for p-J1 and p-J3 ≠ repair of p-J1/2). Repair of long slip-outs was previously demonstrated to be MMR independent (Panigrahi et al., PNAS 107:12593-98) (15). t-tests: (p-J1 vs p-J1/2 $p<0.05$; p-J3 vs p-J1/2 $p<0.05$).